Temperature dependence of coherent oscillations in Josephson phase qubits

J. Lisenfeld[1], A. Lukashenko[1], M. Ansmann[2], J. M. Martinis[2], and A. V. Ustinov[1*]

[1] *Physikalisches Institut III, Universität Erlangen-Nürnberg, D-91058 Erlangen, Germany*
[2] *Department of Physics and California Nanosystems Institute,*
University of California, Santa Barbara, California 93106, USA
(Dated: February 1, 2008)

We experimentally investigate the temperature dependence of Rabi oscillations and Ramsey fringes in superconducting phase qubits driven by microwave pulses. In a wide range of temperatures, we find that both the decay time and the amplitude of these coherent oscillations remain nearly unaffected by thermal fluctuations. The oscillations are observed well above the crossover temperature from thermally activated escape to quantum tunneling for undriven qubits. In the two-level limit, coherent qubit response rapidly vanishes as soon as the energy of thermal fluctuations $k_{\mathrm{B}}T$ becomes larger than the energy level spacing $\hbar\omega$ of the qubit. Our observations shed new light on the origin of decoherence in superconducting qubits. The experimental data suggest that, without degrading already achieved coherence times, phase qubits can be operated at temperatures much higher than those reported till now.

Superconducting qubits are electrical circuits based on Josephson tunnel junctions which are fabricated using techniques borrowed from conventional microelectronic circuits. Between various types of rapidly developing superconducting qubits[1,2,3,4], advantages of Josephson phase qubits are their immunity to charge noise in the substrate and simpler fabrication procedures due to relatively large junction sizes. The experimentally controlled degree of freedom in these devices is the superconducting phase difference across a Josephson junction. By now, several groups succeeded in demonstrating coherent oscillations and quantum state manipulation for phase qubits[5,6,7,8]. A significant increase of the coherence time in phase qubits became possible after systematic research on microscopic defects in insulator materials[9,10,11]. These improvements led to the successful demonstration of quantum state tomography tools for phase qubits[13,14].

The decoherence effects in superconducting qubits give rise to a decay of coherent oscillations in the population of the qubit quantum states. One obvious reason for decoherence in Josephson phase qubits are thermal fluctuations, whose effect has not yet been studied. Most experiments so far have been performed at a base temperature of a dilution refrigerator, typically around 15-30 mK, aiming at the lowest achievable temperature in order to obtain the longest possible coherence times. Higher temperatures remain thus unexplored. It is a common belief that quantum-coherent behavior is limited to temperatures below the crossover temperature T^* between quantum tunneling and thermal activation in a current-biased junction, typically of about 100 mK. In this paper we demonstrate that, in contrast the above expectation, macroscopic quantum coherence can be observed at temperatures much higher than T^* of the junction.

We report here systematic measurements of the temperature dependence of Rabi oscillations and Ramsey fringes in Josephson phase qubits. We present experimental data for samples of different origin and made of
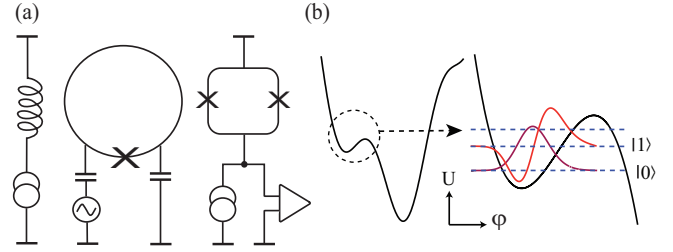

FIG. 1: (a) Schematic of the phase qubit circuit. The qubit junction is embedded in a superconducting loop which is coupled inductively to the flux-biasing coil and readout dc-SQUID. (b) Sketch of the qubit potential $U(\varphi)$. On the right side, a zoom into the shallow left potential well indicates the wave functions describing the two qubit states $|0\rangle$ and $|1\rangle$.

different materials. In a wide range of temperatures, we find that both the decay time and the amplitude of coherent oscillations are rather weakly affected by temperature changes.

A phase qubit uses as its logical quantum states $|0\rangle$ and $|1\rangle$ the lowest two energy eigenstates in a metastable potential well of the Josephson phase in a current-biased junction. An elegant way to decouple the junction from its electromagnetic environment is to apply the bias current through a dc-transformer[9] by embedding the junction in a superconducting loop as shown in Fig. 1(a). The resulting circuit is known as rf-SQUID and has the potential energy

$$U(\varphi) = \frac{\hbar I_C}{2e}\left[1 - \cos\varphi + \frac{1}{2\beta_L}\left(\varphi - 2\pi\frac{\Phi_{\mathrm{ext}}}{\Phi_0}\right)^2\right], \quad (1)$$

where φ is the phase difference across the junction, I_C is its critical current, Φ_{ext} is the externally applied flux through the qubit loop, and Φ_0 is the superconducting flux quantum. The qubit loop inductance L is chosen such that the parameter $\beta_L = 2\pi L I_C/\Phi_0 \approx 4$, result-
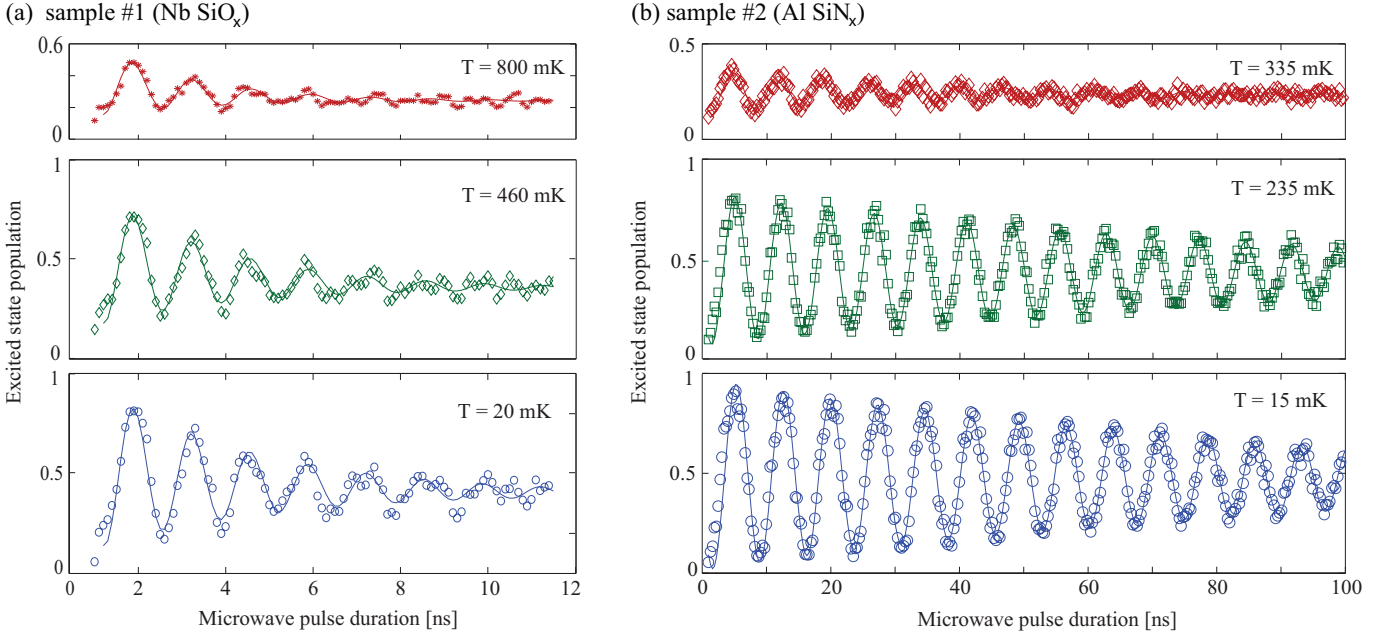
(a) sample #1 (Nb SiO$_x$) (b) sample #2 (Al SiN$_x$)

FIG. 2: (a) Rabi oscillations observed in Nb-based sample #1 with SiO$_2$ insulation and (b) in Al-based sample #2 featuring SiN$_x$ insulation, at the indicated temperatures. Solid lines are a fits to exponentially decaying sine functions from which Rabi amplitude and decay time are extracted.

ing in a double well potential plotted in Fig. 1(b). By adjusting the external magnetic flux close to Φ_0, one of the wells can be made shallow enough to contain only a small number of energy levels. The first excited state $|1\rangle$ in this well can be populated by resonant absorption of photons from the applied microwave field. Reading out the state $|1\rangle$ population is done by using an adiabatic dc-pulse of magnetic flux, which reduces the height of the barrier separating the wells. The pulse amplitude is adjusted such that an inter-well transition occurs only from the excited state. Since the wells differ by the circulation direction of the loop current, the transition from the shallow well to deep well results in a change of magnetic flux, which is registered by recording the switching current of an inductively coupled dc-SQUID.

In our measurements, magnetic flux bias was generated by an on-chip coil coupled weakly to the qubit inductance, while microwave currents were supplied through a coplanar transmission line connected capacitively to the qubit junction. The sample temperature was stabilized in the range between 15 mK and 800 mK. Magnetic shielding was provided by placing the sample in an aluminum-coated copper cell surrounded by a superconducting lead shield and two layers of μ-metal. In order to reduce electromagnetic interference, bias and microwave lines were equipped with cold attenuators, while noise reduction in the dc-SQUID wiring was achieved through capacitively shunted copper-powder filters and current dividers at the 1K pot.

Samples of type #1 have been fabricated according to our design at two different foundries[15,16] by using standard lithographic Nb/AlO$_x$/Nb-trilayer processes. A

Josephson junction of area 7 μm^2 with a current density of 30 A/cm^2 was embedded into a two-turn loop of inductance L=640 pH to form the qubit. All samples of type #1 featured SiO$_2$ as the insulation material between superconducting layers surrounding the junctions. Figure 2(a) shows Rabi oscillations of the excited state population observed by varying the duration of an applied resonant microwave pulse at 16.5 GHz frequency followed by the dc-readout pulse. Fitting the data by an exponentially damped sine function, we extracted Rabi frequency, amplitude and decay time. The T_1 time was obtained by measuring the decay rate of the excited state population after a resonant π-pulse. All measured type #1 phase qubits showed rather short decoherence times. As can be seen in Fig. 2(a), Rabi oscillations have 70% to 80% visibility, decaying at a rate of typically 3 to 5 ns.

In order to observe Rabi oscillation at higher temperatures it is essential to avoid thermal activation out of the shallow potential well. The activation rate increases as the potential barrier height becomes comparable to the thermal energy $k_{\rm B}T$. By reducing the field bias and operating in a deeper potential well, we observed Rabi oscillations in the Nb-based type #1 qubits at temperatures up to 0.9 K. At a temperature of 0.8 K, the amplitude was reduced by a factor of one half, while the oscillation decay time dropped only to 80%. In order to preserve high contrast of the readout at high temperatures we reduced the amplitude of the readout pulse. At high temperature, escape from the excited qubit state to the deep well becomes possible not only by quantum tunnelling but also by thermal activation over the barrier. Moreover, the width of the measured switching-current histogram
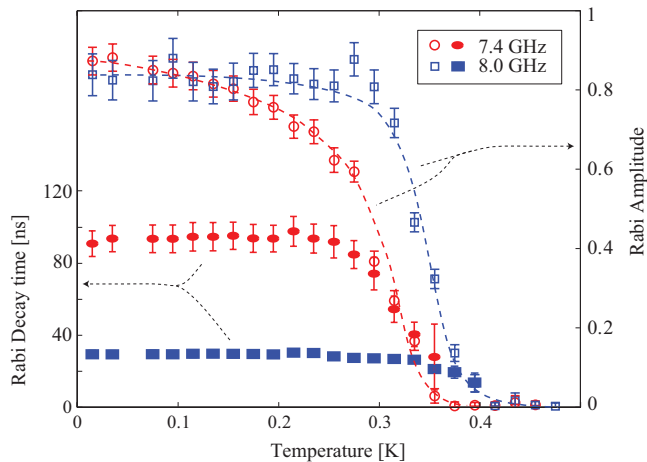
FIG. 3: Amplitude (right axis) and decay time (left axis) of Rabi oscillation observed in sample #2, plotted versus temperature. Dashed lines are guides to the eye.

FIG. 4: Ramsey oscillation amplitude (right axis) and decay time (left axis) vs. temperature (sample # 2). Dashed lines are guides to the eye.

of the readout dc-SQUID increases, which reduces the contrast between the two qubit states. We separated the contributions of the two qubit flux states at high temperatures by a fitting procedure using weighted histograms of the two flux states.

Using the same experimental setup, we have also measured a sample of type #2 containing an Al/AlO$_x$/Al phase qubit fabricated as described in Ref. 13. This qubit features a smaller junction of about 1 μm^2 area which is shunted by a capacitor with SiN$_x$ dielectric layer. It was demonstrated in Ref. 12 that replacing on-chip SiO$_2$ by SiN$_x$ reduces the number of parasitic two-level fluctuators and significantly improves coherence time of the qubit. As it is seen in Fig. 2(b), sample #2 showed Rabi oscillations decay times up to 100 ns – more than one order of magnitude longer than in Nb-SiO$_2$-based samples #1. These data measured in Erlangen are in good agreement with measurements at UC Santa Barbara which were performed using samples of the same batch[13].

In Fig. 3, we plot the temperature dependence of the Rabi oscillation amplitude and decay time for sample #2. For each set of data points, we adjusted the magnetic field bias in order to match the energy level spacing $\Delta E \equiv \hbar\omega$ to be at resonance with the chosen microwave frequency, which is indicated in the legend. The microwave amplitude was chosen to result in Rabi oscillation frequencies of 135 MHz and 205 MHz, respectively for the two data sets at 7.4 GHz and 8.0 GHz driving frequency. Remarkably, increasing the temperature up to about 300 mK, we observed nearly no effect on the oscillation amplitude and decay time. At yet higher temperatures, the oscillations rapidly decay and vanish completely at a temperature $T \approx T_\omega \equiv \hbar\omega/k_B$. The exact T_ω values are 0.355 K at $\omega = 2\pi \cdot 7.4$ GHz and 0.384 K at $\omega = 2\pi \cdot 8.0$ GHz.

To measure the influence of temperature on the dephasing time T_2 in sample #2 we performed a Ramsey-type experiment, in which two $\pi/2$-pulses separated by a
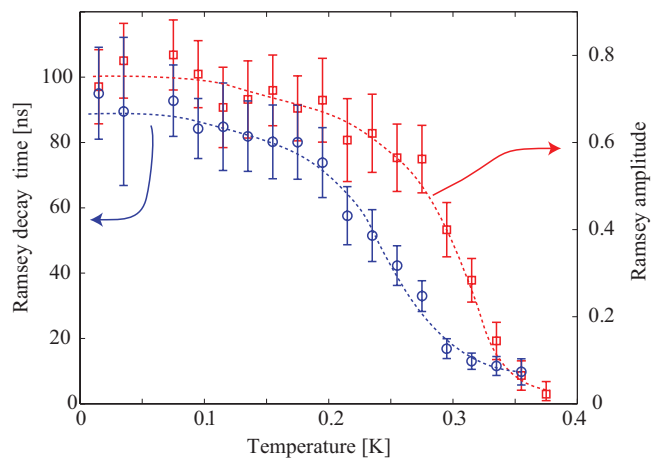
variable duration are applied to the qubit. As expected, the frequency of the observed Ramsey fringes was equal to the detuning of the microwave from the resonance frequency. We took a set of data at 335 MHz detuning from the resonance at 8 GHz. Figure 4 shows the Ramsey oscillation amplitude and the extracted T_2 time versus temperature. At temperatures up to about 180 mK, we measured a weak temperature dependence of the phase coherence time, which at T = 15 mK was $T_2 \approx 90$ ns. At higher temperatures, the time T_2 and fringe amplitude decrease and the oscillations vanish at about 380 mK.

The theoretically expected temperature-induced decay rate from the excited state to the ground state is[17]

$$\Gamma = \frac{2\pi\Delta E}{\hbar} \frac{R_Q}{R} |A_{1,2}|^2 \left[1 + \coth\left(\frac{\Delta E}{k_B T}\right)\right], \quad (2)$$

where $R_Q = h/4e^2$ is the resistance quantum, R is the effective damping resistance, and $A_{1,2} = \langle 0|\frac{\phi}{2\pi}|1\rangle$ is the interaction matrix element between the two states. The temperature dependence of the decay rate is contained in the coth-term and is much less steep than the measured data shown in Fig. 3. We can therefore qualitatively interpret the measured temperature-independent decoherence in our data as limited by microscopic two-level fluctuators at low temperatures. Increasing temperature, on one hand, reduces the fluctuators-induced decoherence as some part of the two-level fluctuators gets saturated by energy absorbed from the thermal bath. On the other hand, high enough temperature leads to conventional decoherence of the qubit described by Eq. (2), which damps coherent oscillations at $T \approx T_\omega$. Detailed theoretical analysis of these competing decoherence mechanisms goes beyond the scope of our experimental work.

To directly measure the energy relaxation time T_1, we applied a resonant microwave π-pulse that prepares the qubit in the excited state. Then, after a variable delay time, we measure the remaining population in the excited

state. We observed exponential decay at half-life times of about 4 ns for sample #1 and about 90 ns for sample #2. The life time T_1 is related to an uncertainty in the energy of the excited state, giving rise to a broadening δE of the level at energy E. Consistent with the measured T_1 relaxation times, we observed a spectroscopic resonance width $\delta\omega$ of about $2\pi\cdot$400 MHz for sample #1 and about $2\pi\cdot$ 10 MHz for sample #2. The measured quality factors $Q = \omega/\delta\omega = E/\delta E$ were about 30 at a transition frequency $\omega_{01} = 2\pi \cdot 16.5$ GHz for the sample #1 and about 600 at a frequency $\omega_{01} = 2\pi \cdot 8$ GHz for sample #2.

The anharmonicity of the qubit potential has the consequence that the separation between adjacent levels decreases with increasing energy. An external microwave will hence be resonant with only one transition if the individual levels are not too broad. This requires a condition

$$\hbar\omega_{12} + \frac{1}{2}(\delta E_1 + \delta E_2) \ll \hbar\omega_{01} \qquad (3)$$

to be satisfied. Here δE_n is the full width of level n arising from its finite lifetime Γ_n^{-1} and ω_{mn} is the transition frequency from level m to level n.

Due to their broad spectroscopic resonance width, our Nb-based qubits of type #1 can not be regarded as two-state systems. The data shown in Fig. 2(a) thus correspond to multilevel dynamics[6,7], which has been recently shown to have its classical counterpart[18,19]. In contrast,

due to the higher Q value of the qubit #2 (of about 600), in this sample we couple by microwaves only the lowest two levels and thus operate this qubit as a two-level system. Deeper potential well in that case remains anharmonic enough not to result in poisoning of the higher levels by microwaves applied at the frequency ω_{01}.

In conclusion, we presented measurements of multi-level Rabi oscillations in low-Q Josephson phase qubits fabricated using standard niobium processes with SiO_2 dielectric. These semi-classical Rabi oscillations persisted at temperatures up to 0.9 K and above, where only a modest decrease in decay time was observed. In contrast, high-Q aluminum-based phase qubits featuring SiN_x can be operated in the two-level limit even at high temperature. Decoherence times measured in these quantum systems depend very weakly on temperature up to the point $T = T_\omega$, where the thermal energy $k_{\mathrm{B}}T$ becomes equal to the energy level separation $\hbar\omega$. Our results demonstrate that, without any significant degradation of their coherence times, the best available phase qubits can be operated at temperatures up to several 100 mK.

* Electronic address: ustinov@physik.uni-erlangen.de
1 Yu. Makhlin, G. Schön, and A. Shnirman, Nature **398**, 305 (1999).
2 M. H. Devoret, A. Wallraff, and J. M. Martinis, cond-mat/0411174.
3 D. Esteve and D. Vion, cond-mat/0505676.
4 G. Wendin and V.S. Shumeiko, cond-mat/0508729.
5 J. M. Martinis, S. Nam, J. Aumentado, and C. Urbina, Phys. Rev. Lett. **89**, 117901 (2002).
6 J. Claudon, F. Balestro, F. W. J. Hekking, and O. Buisson, Phys. Rev. Lett. **93**, 187003 (2004).
7 F. W. Strauch, S. K. Dutta, H. Paik, T. A. Palomaki, K. Mitra, B. K. Cooper, R. M. Lewis, J. R. Anderson, A. J. Dragt, C. J. Lobb, and F. C. Wellstood, cond-mat/0703081.
8 J. Lisenfeld, A. Lukashenko, and A. V. Ustinov, unpublished (2006).
9 R. W. Simmonds, K. M. Lang, D. A. Hite, D. P. Pappas, and J.M. Martinis, Phys. Rev. Lett. **93**, 077003 (2004).
10 K. B. Cooper, M. Steffen, R. McDermott, R. W. Simmonds, S. Oh, D. A. Hite, D. P. Pappas, and J.M. Martinis, Phys. Rev. Lett. **93**, 180401 (2004).
11 J. M. Martinis, K. B. Cooper, R. McDermott, M. Steffen, M. Ansmann, K. Osborn, K. Cicak, S. Oh, D.P. Pappas. R.W. Simmonds and C.C. Yu, Phys. Rev. Lett. **95**, 210503 (2005).
12 R. McDermott, R. W. Simmonds, M. Steffen, K. B. Cooper, K. Cicak, K. Osborn, S. Oh, D. P. Pappas, and J. M. Martinis, Science **307**, 5713 (2005).
13 M. Steffen, M. Ansmann, R. McDermott, N. Katz, R. C. Bialczak, E. Lucero, M. Neeley, E. M. Weig, A. N. Cleland, and J. M. Martinis, Phys. Rev. Lett. **97**, 050502 (2006).
14 M. Steffen, M. Ansmann, R. C. Bialczak, N. Katz, E. Lucero, R. McDermott, M. Neeley, E. M. Weig, A. N. Cleland, and J. M. Martinis, Science **313**, 1423 (2006).
15 Hypres Inc., Elmsford, N.Y., USA.
16 VTT Technical Research Center, Finland.
17 A. J. Legget, S. Chakravarty, A.T. Dorsey et. al., Rev. Mod. Phys. **59**, 1 (1996).
18 N. Grønbech-Jensen and M. Cirillo, Phys. Rev. Lett. **95**, 067001 (2005).
19 J. E. Marchese, M. Cirillo, and N. Grønbech-Jensen, Phys. Rev. B **73**, 174507 (2006).